New hydrophobic deep eutectic solvent for electrochemical applications

Nesrine Chaabene, Kieu Ngo, Mireille Turmine, Vincent Vivier

NEW HYDROPHOBIC DEEP EUTECTIC SOLVENT FOR ELECTROCHEMICAL APPLICATIONS

NESRINE CHAABENE, KIEU NGO, MIREILLE TURMINE, VINCENT VIVIER

Sorbonne Université, CNRS, Laboratoire Interfaces et Systèmes Electrochimiques, LISE, F-75005 Paris, France

Abstract

Deep eutectic solvents (DESs) are known as cheap and biodegradable solvents which are easier to synthesize than ionic liquids (ILs). In this work, a new hydrophobic DES based on menthol is described. It consisted in a mixture of menthol and acetic acid in which ethanolamine has been added in order to increase the conductivity up to few $mS.cm^{-1}$. The physicochemical properties as a function of temperature, in the range of 293 to 333 K, of this menthol-based DES have been compared to the ethaline, which is one of the most widely used DES. Cyclic voltammetry has been used to study the electrochemical behavior of an electroactive mediator, the hydroxymethylferrocene (FcMeOH), which is a reversible electrochemical system and its diffusion coefficient, determined in both DESs, is of the same order of magnitude than the one reported for the 1-ethyl-3-methylimidazolium bis(trifluoro-methanesulfonyl)imide (EMIMTFSI), which is the most widely used IL for electrochemical applications. This new class of DES thus provide an eco-friendly alternative for electrochemical applications.

Keywords: *menthol-based DES; hydrophobic solvent; biodegradable solvent; cyclic voltammetry*

Corresponding author:

Mireille Turmine: mireille.turmine@sorbonne-universite.fr

1. Introduction

With the emergence of green chemistry, ionic liquids (ILs) are currently used as an attractive alternative to organic solvents [1, 2]. Despite their many interesting physicochemical properties such as a low melting temperature (< 100 °C), a high thermal stability, a low vapor pressure, a non-flammability and a wide electrochemical potential window, ILs remain expensive and their preparation can be relatively complex [3, 4]. Recently, deep eutectic solvents (DESs) have been used as analogues and alternative green solvents to replace traditional solvents but also to take advantage of some of the most prominent properties of ILs [5, 6]. They are generally composed of at least two compounds bonded together by intermolecular forces such as hydrogen bonding. These interactions result in a significant decrease in the melting point of the mixture, DESs often becoming liquid at room temperature. Additionally, DESs have many advantages. For example, they can be easily synthesized with a high purity at low cost, and their components are biodegradable and have a low toxicity [7].

The first DESs described in the literature [8] are based on choline chloride and urea or ethylene glycol, known as reline or ethaline, respectively. Even if choline chloride is one of the most widespread components used for DESs [9-11], the presence of chloride may be a limiting factor for applications in electrochemistry. Moreover, most of these choline-based DES media suffer from their hydrophilicity. Interestingly, the almost unlimited number of possible combinations offers an infinite range of DESs that can be custom-synthesized depending on the targeted application [12] and it should also be mentioned that some DESs can be obtained by the mixing of both ionic and non-ionic species.

Recently, the group of Marrucho [13, 14] has reported a new hydrophobic DES prepared from menthol and an organic acid, which is used for the extraction of different biomolecules such as caffeine, tryptophan, isophthalic acid, and vanillin from the aqueous phase to the eutectic mixture phase. This new family of DESs should thus offer new perspectives for electrochemical applications, but unfortunately these DESs have a poor ionic conductivity.

The main objective of this work is to investigate the preparation of a new DES based on the mixture of menthol and carboxylic acid in which an amine has been added in order to increase the conductivity up to few $mS.cm^{-1}$, while still keeping the environmentally-friendly and bio-compatible characters of the end solvent. Such a new hydrophobic DES should thus be a good candidate as a new electrolyte for electrochemical applications.

First, the physicochemical properties of this DES including density, viscosity, conductivity and electrochemical windows have been studied and compared to a usual DES (*i.e.* ethaline) and common hydrophobic ionic liquid (*i.e.* EMIMTFSI). Then, its use as solvent for electrochemical application has been investigated by cyclic voltammetry in presence of an electroactive probe, namely the hydroxymethylferrocene (FcMeOH).

2. Experimental section

2.1 Chemicals and synthesis of DESs

Choline chloride (ChCl) (Acros Organics, purity ≥ 99%), ethylene glycol (EG) (VWR Chemical, purity ≥ 99%), DL-Menthol (Sigma Aldrich, purity ≥ 95%), ethanolamine (Sigma Aldrich, purity ≥ 98%) and acetic acid (Sigma Aldrich, purity ≥ 99.7%) were used as received. The chemical structures of the compounds used for the synthesis of DESs are presented in Fig. 1.

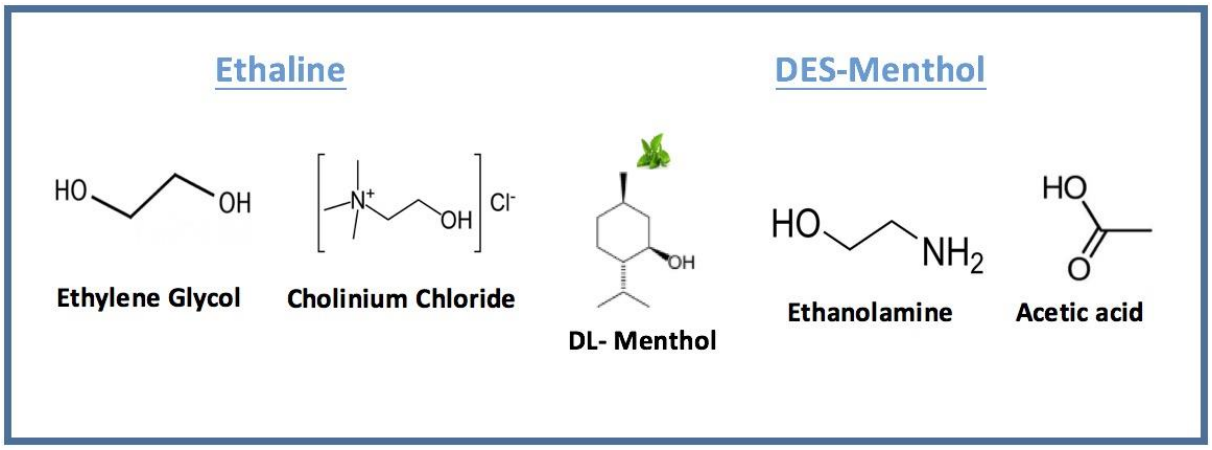

Figure 1. *Chemical structures of the compounds used for the preparation of deep eutectic solvents studied in this work.*

1-ethyl-3-methylimidazolium bis(trifluoromethanesulfonyl)imide (EMIMTFSI) was synthesized according to the method previously described in the literature [15]. Its structure was checked by ^{1}H NMR spectroscopy and ElectroSpray mass spectroscopy. ^{1}H NMR spectroscopy (400 MHz, $CDCl_3$, δ/ppm relative to TMS), δ = 8.60 (s, 1H), 7.41(d, 2H, *J*=10.3), 4.25 (q, 2H, *J*=7.36), 3.93(s, 3H), 1.54(t, 3H, *J*=7.4). Electrospray mass spectroscopy (ESI positive): *m/z* = 111.1 ($EMIM^+$); (ESI negative) *m/z* = 280.1 ($TFSI^-$). The estimated purity is about 99%.

Ethaline was prepared by mixing cholinium chloride with ethylene glycol with a 1:2 molar ratio. The mixture was stirred for 3 hours at room temperature to yield a homogeneous and transparent liquid. The menthol-based eutectic mixture was prepared by mixing menthol, ethanolamine and acetic acid in a 1:2:4 molar ratio. The mixture of these three compounds was then heated at 80 °C for 30 min and then slowly cooled down until reaching room temperature leading to a homogeneous transparent liquid. The water content in the three freshly prepared solvent was titrated using a Karl – Fisher coulometer (C20, Mettler Toledo). Thus, the water content of the hydrophobic ionic liquid (EMIMTFSI) was 50 ppm, that of menthol-based DES was 85 ppm while the amount of water in ethaline was about 2000 ppm.

The hydrophobicity test was performed in order to characterize the role of menthol (Fig. 2) by comparing two mixtures. The first one was a mixture of ethanolamine and acetic acid in a 2:4 molar ratio. The second mixture was the as-prepared menthol-based eutectic solvent. The same amount of water (5 mL) was mixed with both mixtures, which resulted in the formation of two phases in the case of the menthol-based eutectic mixture (Fig. 2a), whereas the acetic acid – ethanolamine mixture mixed up with water (Fig. 2b).

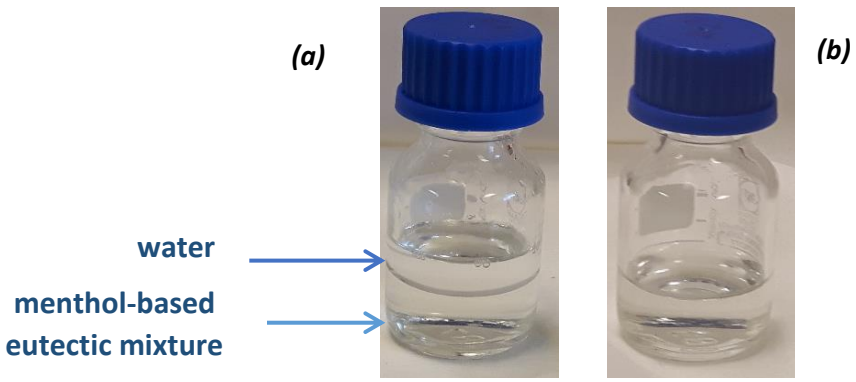

Figure 2: *Hydrophobicity test for menthol-based eutectic solvent (a), and acetic acid – ethanolamine mixture (b)*

2.2 Physicochemical characterization of the solvents

The density, viscosity and ionic conductivity of all the solvents were measured using the devices listed in Table 1, in which the estimation of the average uncertainty for each physicochemical property is also reported.

Table 1. *Device and uncertainty for physical-chemical property measurements*

Physicochemical property	Measurement device	Standard uncertainty
Density	Anton Paar DMA 5000	Less than 0.05 kg m^{-3}
Viscosity	Anton Paar Lovis 2000M/ME	Less than 0.5 %
Conductivity	Radiometer MeterLab CDM 230	1 %

Density measurements were conducted using a vibrating-tube densimeter DMA 5000 M (Anton Paar) in the temperature range from 293.15 to 333.15 K. The apparatus was calibrated using the extended calibration procedure with dry air and degassed ultra-pure water (Elga, Veolia) with an electrolytic conductivity equals 0.055µS cm^{-1} at 298.15 K. With regard to the viscosity-related errors, an automatic correction was done using the instrument by measuring the damping effect of the sample followed by a mathematical correction of the density. These measurements were performed with an uncertainty of less than ±0.05 kg m^{-3}, whereas repeatability is estimated to be ±0.005 kg m^{-3}. Temperature was measured with an uncertainty of ±0.02 K and a resolution of ±0.001 K.

The kinematic viscosity, ν, of the investigated systems was determined with a calibrated and thermostated rolling-ball viscometer (Lovis 2000 M, Anton Paar), which measures the rolling time of a ball through transparent and opaque liquids according to Hoeppler's falling-ball principle. The microviscometer is equipped with three calibrated glass capillaries of different diameter (1.59, 1.8 and 2.5) mm and steel balls. The dynamic viscosity, η, is obtained by measuring the time taken by the steel ball to fall from one side to the end of the capillary filled with the sample at a certain angle and temperature, and by knowing the density of the sample. The calibration of the capillaries was done using viscosity standards provided by the manufacturer and with water. The viscosity was measured with accuracy better than ±0.5% (with the same ball and depending on the size of the capillary and the temperature). The viscosities were conducted in the temperature range from 293.15 to 333.15 K, and the accuracy of the temperature measurements was ±0.02 K.

The ionic conductivity, s, was measured using a CDM 230 Conductivity Meter from MeterLab™, Radiometer analytical operating at five different frequencies (94 Hz, 375Hz, 2.93kHz, 23.4kHz and 46.9kHz, depending of the conductance range) with an estimated uncertainty of 1%. The conductivity cell was a Radiometer Analytical CDC741T-6 with temperature sensor (2-pole Pt sensor, K=1.0 cm^{-1}, glass body). Temperature and data

acquisitions were made by a personal computer connected to the conductivity meter. The experimental cell was calibrated with standard 0,1 mol.L^{-1} KCl solution, and the resulting cell constant was 1.0358 cm^{-1}. The temperature of the samples was controlled using cryothermostat polystat with thermal stability ± 0.03 K. The sample was allowed to spend about 20 min at constant temperature before performing any single measurement, while 40 min at the phase transition.

All the electrochemical measurements were performed with a three-electrode cell using a GAMRY REF600 potentiostat. A home-made gold microelectrode of 200 µm in diameter was used as working electrode and a platinum grid of 1x1 cm^2 was used as counter electrode. The reference electrode was based on the Ag^+ / Ag electrode in a double junction compartment. It consists of a silver wire immersed in a first junction containing a saturated solution of silver nitrate ($AgNO_3$) in DES, with a sintered glass at the bottom. A second junction containing pure DES was used to prevent the working solution in the main electrochemical compartment from any contamination of ions (Ag^+ and NO_3^-) coming from the first junction containing the reference electrode. Before each experiment, the working electrode was carefully cleaned by mechanical grinding with a SiC paper (P4000) followed by an electrochemical cycling in a 0.1 mol L^{-1} sulfuric acid aqueous solution by sweeping the potential between -1 and 1.3 V/SCE at 100 mV.s^{-1} for 10 min.

All the electrochemical experiments were performed under a dry argon atmosphere to avoid the presence of oxygen and air humidity. All experiments were performed three times.

3. Results and discussions

3.1 Physicochemical properties

Variations of the density, viscosity and conductivity of the menthol-based DES and ethaline were plotted as a function of temperature (in the range 293K - 333K) at atmospheric pressure on Fig. 3. The temperature dependence of these properties was gathered in Table 2 for menthol-based DES. As shown on Fig. 3, the density, viscosity and conductivity values of ethaline are close to some of those reported in the literature [16-21]. For a better comparison, the values (from this study and from the literature) of the physicochemical parameters of ethaline have been presented in Table S1. As previously mentioned by some previous work [18, 22], a disparity in the thermophysical properties of DES exists by comparing the different values even from a same group of researchers. This discrepancy can be due to the operating conditions or the water content into the mixtures.

Table 2. *Values of some physicochemical parameters of EMIMTFSI at different temperatures at pressure (p= 0.1 MPa)*

T (K)	density (ρ in g.cm^{-3})	viscosity (η in mPa.s)	conductivity (σ in mS.cm^{-1})
293.15	1.049065	211.70	0.545
298.15	1.045406	145.82	0.688
303.15	1.041785	103.64	0.854
308.15	1.038154	75.93	1.023
313.15	1.034511	57.13	1.215
318.15	1.030862	43.83	1.430
323.15	1.027218	34.41	1.657
328.15	1.023572	27.56	1.885
333.15	1.019928	22.44	2.180

The density of both DESs decreases linearly when the temperature increases (Fig3.a), due to the molar volume increase leading to a decrease in the average distance between the molecules [23]. From the density measurements, the thermal-expansion coefficient, α, can be calculated according to

$$\alpha = \frac{1}{V}\left(\frac{\partial V}{\partial T}\right)_p = -\frac{1}{\rho}\left(\frac{\partial \rho}{\partial T}\right)_p \quad (1)$$

Where V is the molar volume of the DES and T, the temperature. This thermal expansion coefficient is related to the change in volume of the medium with the temperature as shown in Eq. 1, and can be linked to the free volume in the solvent. The higher the thermal expansion coefficient, the higher the free volume. To determine these thermal expansion coefficients, the logarithm of the density ($ln\ \rho$) was plotted against the temperature. A straight-line was obtained for the both DESs as shown on Fig. 3d. The slope corresponds to the thermal expansion coefficient. Table 3 gives the coefficients of thermal expansion of both DESs which were compared to the values of a common hydrophobic IL (EMIMTFSI) [24]. Similarly to imidazolium based ionic liquids, both DESs are less compressible that common organic solvents [25, 26] as toluene (11.29 10^{-4} K^{-1} at 298.15K), dichloromethane (13.5 10^{-4} K^{-1} at 298.15K) or ethanol (10.9 10^{-4} K^{-1} at 298.15K).

It can also be noticed that the thermal expansion coefficient value of the ternary mixture based on menthol is lower than the one for the binary menthol – acetic acid studied by Ribiero et al. [14] (7 10^{-4} K^{-1} for this work compared to 9.1 10^{-4} K^{-1} for the binary mixture). The addition of ethanolamine to the menthol based-DES decreases the free volume thus leading to a less compressible solvent.

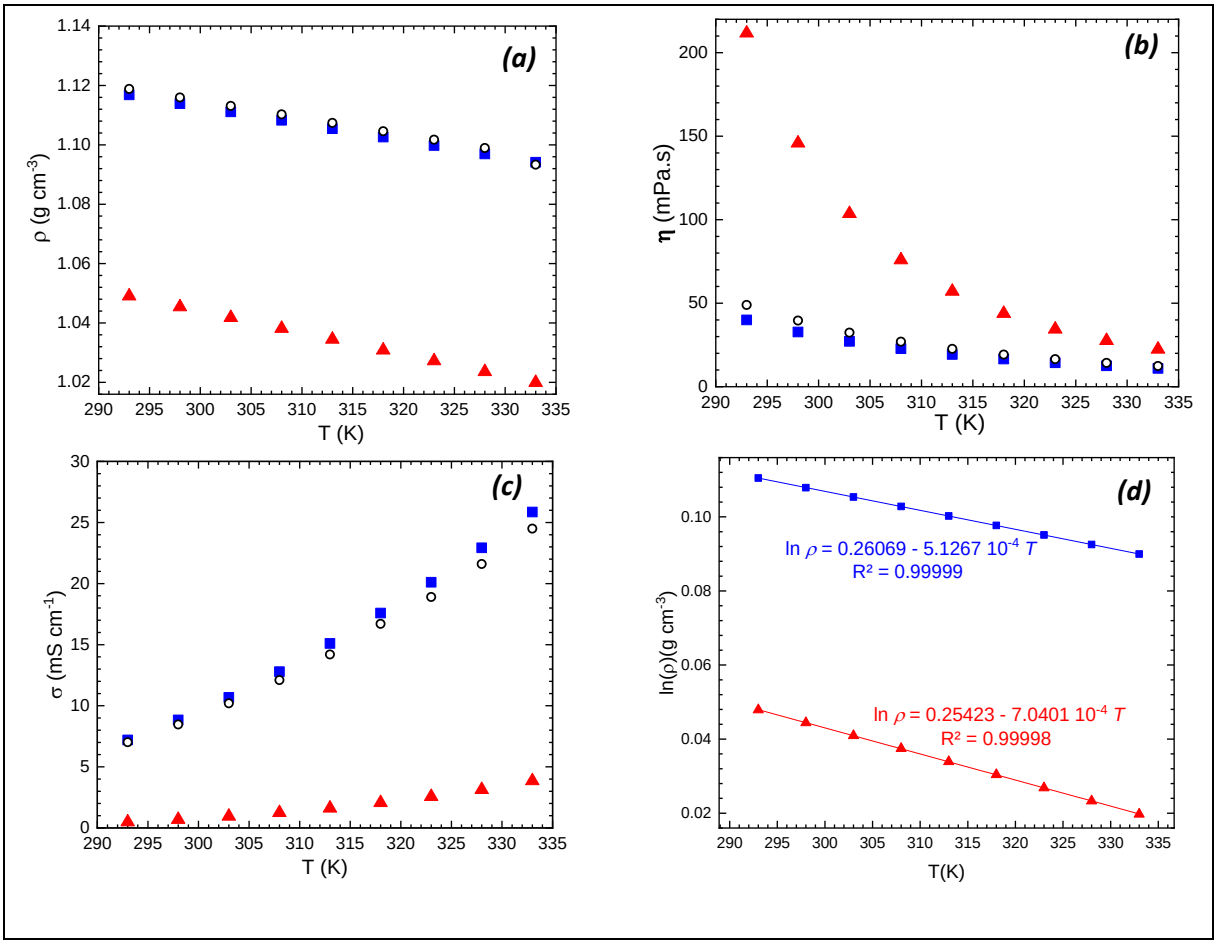

Figure 3. *Variations of (a) the density, (b) the viscosity, (c) the conductivity and (d) the logarithm of the density as a function of the temperature of the DESs - ethaline (blue squares); ethaline from ref. [18] (black circles); and DES-Menthol (red triangles).*

The dynamic viscosity, η, defines the internal resistance of a fluid to a shear stress. The knowledge of its value is of interest for electrochemical applications due to its strong effect on the mass transport properties in the solution that significantly affects the diffusion of electroactive species in the media. The variations of the DES viscosity as a function of the temperature are reported in Fig. 3b. This viscosity profile is similar to what is usually observed in the literature for DES mixtures [7, 27, 28], with a more or less marked exponential decrease of the viscosity with the increase of the temperature. In a DES, the viscosity is mainly related to the formation of hydrogen bonds and van der Waals interactions. Menthol-based DES

exhibits higher viscosity than ethaline. For example, at 298 K, the viscosity of menthol-based DES is 145 mPa.s, that is, about four times larger than viscosity of ethaline (33 mPa.s) at the same temperature. Such a high viscosity for menthol-based DES may be ascribed to the presence of a strong hydrogen-bond network between all the components.

The temperature dependence of the viscosity values is most often fitted using an Arrhenius-like relationship, which expresses as

$$ln\,\eta = ln\,\eta^{\infty} + \frac{E_{\eta}}{RT} \quad (2)$$

Where E_{η} is the activation energy, η the viscosity, η^{∞} the pre-exponential factor and R the perfect gas constant. E_{η} is the energy barrier that must be overcome by the ions to move through the medium. The larger E_{η}, the harder for the ions to move in the liquid. This equation is based on the empirical relationship of Arrhenius for the temperature dependence of reaction rates. Most of the time, Eq.2 can be applied to describe the temperature dependence of the viscosity in a narrow temperature range. For larger temperature range, another empirical approach the so-called Vogel-Tamman-Fulcher (VTF) relationship is commonly used to describe this temperature dependence [29]. In parallel, in order to give a better understanding of the viscous flow with a thermodynamic light, many authors rely on the Eyring's transition state theory applied to the viscosity [30]. In this approach, the viscosity of a liquid is given by

$$\eta = \frac{h\mathcal{N}_a}{V} exp\left(\frac{\Delta G^{\neq}}{RT}\right) \quad (3)$$

where $\Delta G^{\neq}$ is the molar Gibbs free energy of activation of the viscous flow, h the Planck's constant, $\mathcal{N}_a$ the Avogadro's number and V the molar volume of the liquid, which can be expressed as,

$$V = \frac{M}{\rho} \quad (4)$$

with ρ the density of the considered DES and M its molar mass.

From Eq. 3 the following expanded relation is obtained

$$ln\,\eta = ln\left(\frac{h\rho\mathcal{N}_a}{M}\right) - \frac{\Delta S^{\neq}}{R} + \frac{\Delta H^{\neq}}{RT} \quad (5)$$

Where $\Delta H^{\neq}$ and $\Delta S^{\neq}$ are the enthalpy and entropy of activation, respectively. By comparison of Eq. 2 and Eq. 5, it comes

$$\eta^{\infty} = \frac{h\rho\mathcal{N}_a}{M} exp\left(-\frac{\Delta S^{\neq}}{R}\right) \quad (6)$$

and

$$E_{\eta} \approx \Delta H^{\neq} \quad (7)$$

Eq. 6 shows why some authors introduce the pre-exponential factor of the Arrhenius-like relation as an entropic term. This also shows that Eq. 2 can be modelled by a straight-line only for narrow temperature range, which widely depends on the variation of the density with the temperature. Thus, $E_{\eta} = \Delta H^{\neq}$ only if the density can be considered as constant in the investigated temperature range. Nevertheless, by plotting $ln\left(\frac{M\eta}{h\rho\mathcal{N}_a}\right)$ as a function of T^{-1} for the studied DES, $\Delta H^{\neq}$ and $\Delta S^{\neq}$ were determined and presented in Table 3, with the value of E_{η} determined from Eq. 2. As expected, the activation energy is very close to the enthalpy of activation. Moreover, the values of activation entropy are of interest. As shown in Table 3, DES-menthol has the highest activation entropy when compared to both ethaline and EMIMTFSI: indeed, DES-menthol contains the larger number of compounds.

Table 3. *Characteristic parameters for density, viscosity and conductivity variations of the DESs and EMIMTFSI determined from their variations as a function of the temperature*

Medium	M (/g mol^{-1})	α (/10^{-4} K^{-1})	E_{η} (/kJ mol^{-1})	E_{σ} (/kJ mol^{-1})	$\Delta H^{\neq}$ (/kJ mol^{-1})	$\Delta S^{\neq}$ (/J K^{-1} mol^{-1})
Ethaline	87.7	5.1	26.2	25.9	25.8	13.6
DES-Menthol	74.1	7.0	45.4	41.6	44.8	66.0
EMIMTFSI*	391.3	6.6	23.4	20.8	22.8	-5.5

*from ref [24]

Fig. 3c shows that the conductivity of both DESs increases almost linearly with the temperature. This is a direct consequence of a faster movement of ions in the media at higher temperatures. At room temperature, the conductivity of ethaline is about 8.8 mS.cm^{-1}, which is more than one order of magnitude higher than the conductivity measured for the menthol-based DES (0.7 mS.cm^{-1}). Such a difference may be ascribed, at least partially, to the higher viscosity of the

menthol-based DES. The conductivity of an ion, σ_i, is linked to its diffusion coefficient, D_i, as expressed by the Nernst-Einstein equation,

$$\sigma_i = \frac{c_i z_i^2 \mathcal{F}^2 D_i}{RT} \quad (8)$$

where c_i stands for the concentration of the ion i and z_i its charge. Usually, the diffusion coefficient is linked to the viscosity by the Stokes-Einstein relation, defined for a model spherical species i of an effective radius r_i, as

$$D_i = \frac{k_B T}{6\pi r_i \eta} \quad (9)$$

This relation is commonly used to determine the diffusion coefficient of species in IL. However, this latter equation is only valid if the ion i is bigger than the species constituting the medium, but there are other relations linking the diffusion coefficient to the reverse of the viscosity taking into account, for example, the different characteristic lengths between the species [31]. Anyhow, we have to keep in mind that the diffusion coefficient is inversely proportional to the viscosity. By taking account Eqs. 8 and 9, the conductivity of an ion can be expressed as

$$\sigma_i = \frac{c_i z_i^2 \mathcal{F}^2}{6\pi \mathcal{N}_a r_i \eta} \quad (10)$$

The conductivity of the mixtures is the sum of ionic conductivities of the anion and the cation.

$$\sigma = \sigma_{anion} + \sigma_{cation} = \frac{\mathcal{F}^2}{6\pi \mathcal{N}_a \eta}\left(\frac{c_{anion} z_{anion}^2}{r_{anion}} + \frac{c_{cation} z_{cation}^2}{r_{cation}}\right) \quad (11)$$

In our case, $c_{anion} = c_{cation} = c_{salt}$, then

$$\sigma = \frac{\mathcal{F}^2}{6\pi \mathcal{N}_a \eta} \frac{x_{salt}}{M} \rho \left(\frac{1}{r_{anion}} + \frac{1}{r_{cation}}\right) \quad (12)$$

x_{salt} is the molar fraction of the salt in the mixture, ($x_{salt} = 1$, for neat IL). Combining Eq. 12 with Eq. 2, an Arrhenius-like relationship is obtained

$$ln\ \sigma = \ln \sigma^{\infty} - \frac{E_\sigma}{RT} \quad (13)$$

Where σ^{∞} is a constant and E_σ is the activation energy for ionic conductivity. E_σ of the DESs and EMIMTFSI determined from the experimental data using Eq. 13 are shown in Table 2.

By considering, Eqs. 5 and 13, the following expression is then obtained

$$ln\ \sigma = ln\left(\frac{\mathcal{F}^2 x_{salt}}{6\pi \mathcal{N}_a{}^2 h}\left(\frac{1}{r_{anion}}+\frac{1}{r_{cation}}\right)\right)+\frac{\Delta S^{\neq}}{R}-\frac{\Delta H^{\neq}}{RT} \qquad (14)$$

Knowing the activation entropy and enthalpy, only the sum $\left(\frac{1}{r_{anion}}+\frac{1}{r_{cation}}\right)$ can be calculated. As shown in table 3, this value decreases as the temperature increases.

Table 3. *Variation of the sum* $\left(\frac{1}{r_{anion}}+\frac{1}{r_{cation}}\right)$ *as a function of the temperature*

Temperature (/K)	ethaline $\sum_i \frac{1}{r_i}$ (/m)	DES-Menthol $\sum_i \frac{1}{r_i}$ (/m)	EMIMTFSI* $\sum_i \frac{1}{r_i}$ (/m)
293	$9.07\ 10^9$	$3.23\ 10^9$	$5.32\ 10^9$
298	$8.30\ 10^9$	$3.00\ 10^9$	$5.44\ 10^9$
303	$7.61\ 10^9$	$2.76\ 10^9$	$5.49\ 10^9$
308	$7.02\ 10^9$	$2.48\ 10^9$	$5.44\ 10^9$
313	$6.47\ 10^9$	$2.23\ 10^9$	$5.35\ 10^9$
318	$5.96\ 10^9$	$2.00\ 10^9$	$5.23\ 10^9$
323	$5.44\ 10^9$	$1.78\ 10^9$	$5.09\ 10^9$
328	$5.01\ 10^9$	$1.57\ 10^9$	$4.96\ 10^9$
333	$4.60\ 10^9$	$1.42\ 10^9$	$4.93\ 10^9$

*from ref [24]

For these three media the ions are different as well as their environment. At this stage, the analysis of these data is difficult. Indeed, first, it is necessary to check that the hypothesis of Stokes-Einstein concerning the size of the ions is always valid. Afterwards, we need an assumption or other analysis or calculation to differentiate the anion from the cation. For EMIMTFSI, the cation radius can be evaluated by taking the anion radius available in the literature [32, 33], r_{TFSI} = 3.65 Å. Thus, at 298K, the radius of the cation EMIM is around 3.7 Å. For DES, to our knowledge, there is no value for ionic radius, since the environment is very different, we chose to only calculate an average radius at 298K to compare these two different mixtures. At 298 K, the average radius is about 2.4 Å in ethaline and 6.7 Å in menthol-based DES.

297

298 *3.2 Electrochemical properties*

299 Before envisioning any practical electrochemical application, it is of interest to determine the
300 electrochemical window (EW) of the solvents. Figs. 4a and b show the EW of each DES
301 measured using linear sweep voltammetry (LSV) from -2.5 to 2 V/Ag^+/$AgNO_3$ using a 200 µm
302 in diameter gold electrode. Unlike aprotic ionic liquids, which usually have broad
303 electrochemical windows spreading over 4 to 5 V [34], the DESs studied in this work display a
304 lower electrochemical stability comprised in the range 2 to 2.5 V (taking a cutoff value for the
305 current density of ±100 µA cm^{-2}). However, this EW is twice larger than the EW of water
306 electrolyte, which makes these DESs attractive for electrochemical applications.

307 The electrochemical behavior of an electroactive species, the hydroxymethylferrocene
308 (FcMeOH), in DES_s was then studied by cyclic voltammetry (CV) by varying the scan rates
309 (Fig. 4c). CVs clearly exhibit a quasi-reversible behavior, in which the ratio between the current
310 density of the anodic peak j_{pa} and that of the cathodic peak j_{pc} is close to 1 also at low scan rates
311 whereas the difference between the anodic and cathodic peak potentials is in agreement with
312 the predicted values ($E_{pa} - E_{pc} \approx 60$ mV) for a mass-transfer controlled system [35]. The current
313 density peak (j_{p1}) varies linearly with the square root of the scan rate (Fig. 4d) showing that the
314 mass transfer of FcMeOH in the investigated DESs is controlled by the diffusion of
315 electroactive species [35].

316

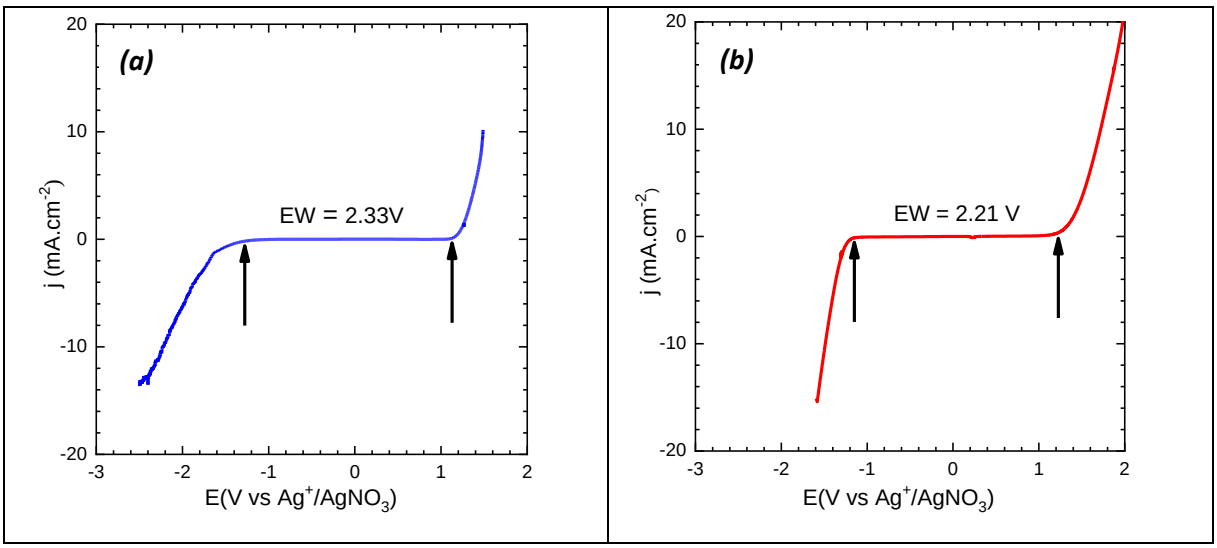

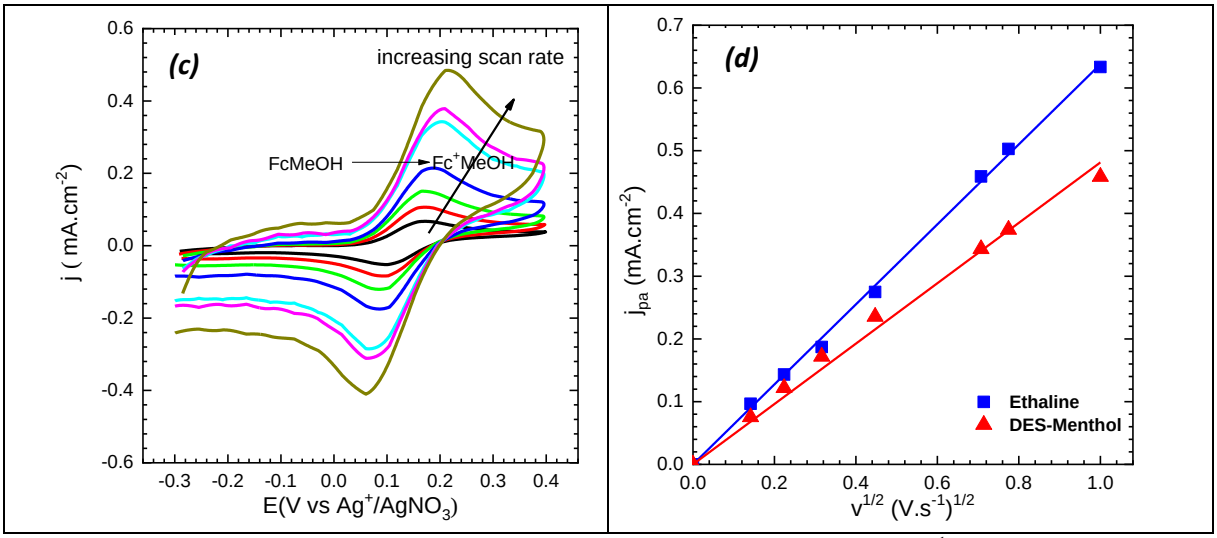

Figure 4. *LSV of (a) ethaline and (b) DES-Menthol at a scan rate of 5mVs^{-1}; (c) CV of a 5mM FcMeOH in menthol-based DES at different scan rates (from 20 to 1000mVs^{-1}); (d) variation of the current density peak j_{pa} with the square root of the scan rate for the FcMeOH oxidation in DES. All these experiments were performed, at (25 ± 0.1)°C, with a gold working electrode (200 µm in diameter).*

On this scan rate domain, the diffusion coefficient of FcMeOH can thus be obtained from the slope of the current intensity curve as a function of square root of sweep rate by using Randles-Sevick equation

$$i_p = 0.446n\mathcal{F}\sqrt{\frac{n\mathcal{F}v}{RT}}C_i A\sqrt{D_i} \qquad (15)$$

where i_p is the current of the peak, n the number of electron exchanged, A the electrode surface area, $\mathcal{F}$ the Faraday constant, D_i the diffusion coefficient, C_i the concentration of the electroactive species i, and v the scan rate.

Table 4 *Variation of the diffusion coefficient of ferrocene methanol as a function of the viscosity of the medium*

Medium @298K	η (/mPa.s)	D (/10^{-7}cm^2.s^{-1})
EMIMTFSI*	30.4	3.5
Ethaline	32.7	2.2
DES-Menthol	146	1.1

*from ref [24]

The diffusion coefficients values of FcMeOH in DESs are presented in Table 3. It should be noticed that the diffusion coefficients obtained in DESs are of the same order of magnitude than those obtained in the pure ionic liquid (*e.g.* EMIMTFSI). In ethaline the diffusion coefficient of FcMeOH is twice than in the menthol-based DES. Indeed, as shown in Table 4, ethaline has a lower viscosity, which explains the more efficient mass transport corresponding to higher value of the diffusion coefficient. Interestingly, the diffusion coefficient of FcMeOH is of the same order of magnitude in the DESs and IL studied in this work, showing the great potentials of the new menthol-based DESs.

4. Conclusions

Two deep eutectic solvents (DESs), ethaline and menthol-based DES, have been prepared and characterized. Hydrophobicity test was performed to show the role of menthol in the mixture. The addition of ethanolamine to the menthol – acetic acid mixture leads to an increase of the conductivity. Their physicochemical properties including density, viscosity and conductivity were studied in detail at different temperatures. Although these mixtures are no conventional, we estimated an average radius of the ions assuming that the Stokes-Einstein relationship can be applied.

LSV curves at low scan rate allowed obtaining the electrochemical window of DESs. The electrochemical windows of the two DESs do not show significant differences and are about 2.4 V. The redox couple $FcMeOH^+$/FcMeOH is reversible in menthol-based DES and the diffusion coefficient of FcMeOH is of the same order of magnitude as that obtained in the pure ionic liquid (EMIMTFSI), thus showing than this DES is suited for performing electrochemical experiments.

Menthol-based DESs are thus a good alternative to hydrophobic ionic liquid for electrochemical applications (*e.g.* for battery application) especially since it is a biocompatible solvent, easy to synthesize and cheap.

Acknowledgements

This work was supported by the Ecole Doctorale Chimie Physique et Chimie Analytique de Paris Centre (ED 388).

References

[1] M. Armand, F. Endres, D.R. MacFarlane, H. Ohno, B. Scrosati, Ionic-liquid materials for the electrochemical challenges of the future, Nat Mater 8 (2009) 621-629.

[2] V.L. Martins, R.M. Torresi, Ionic liquids in electrochemical energy storage, Curr. Opin. Electrochem. 9 (2018) 26-32.

[3] Y. Hu, Z. Wang, X. Huang, L. Chen, Physical and electrochemical properties of new binary room-temperature molten salt electrolyte based on LiBETI and acetamide, Solid State Ionics 175 (2004) 277-280.

[4] S.B. Capelo, T. Mendez-Morales, J. Carrete, E. Lopez Lago, J. Vila, O. Cabeza, J.R. Rodriguez, M. Turmine, L.M. Varela, Effect of temperature and cationic chain length on the physical properties of ammonium nitrate-based protic ionic liquids, J. Phys. Chem. B 116 (2012) 11302-11312.

[5] E.L. Smith, A.P. Abbott, K.S. Ryder, Deep eutectic solvents (DESs) and their applications, Chem. Rev. 114 (2014) 11060-11082.

[6] C.J. Clarke, W.C. Tu, O. Levers, A. Brohl, J.P. Hallett, Green and Sustainable Solvents in Chemical Processes, Chem. Rev. 118 (2018) 747-800.

[7] M.A. Kareem, F.S. Mjalli, M.A. Hashim, I.M. AlNashef, Phosphonium-Based Ionic Liquids Analogues and Their Physical Properties, J. Chem. Eng. Data 55 (2010) 4632-4637.

[8] A.P. Abbott, G. Capper, D.L. Davies, R.K. Rasheed, V. Tambyrajah, Novel solvent properties of choline chloride/urea mixtures, Chem Commun (Camb) (2003) 70-71.

[9] A.P. Abbott, D. Boothby, G. Capper, D.L. Davies, R.K. Rasheed, Deep eutectic solvents formed between choline chloride and carboxylic acids: Versatile alternatives to ionic liquids, J. Am. Chem. Soc. 126 (2004) 9142-9147.

[10] C. Teja, F.R. Nawaz Khan, Choline Chloride-Based Deep Eutectic Systems in Sequential Friedlander Reaction and Palladium-Catalyzed sp(3) CH Functionalization of Methyl Ketones, ACS Omega 4 (2019) 8046-8055.

[11] A. Yadav, S. Pandey, Densities and Viscosities of (Choline Chloride + Urea) Deep Eutectic Solvent and Its Aqueous Mixtures in the Temperature Range 293.15 K to 363.15 K, J. Chem. Eng. Data 59 (2014) 2221-2229.

[12] Q.H. Zhang, K.D. Vigier, S. Royer, F. Jerome, Deep eutectic solvents: syntheses, properties and applications, Chemical Society Reviews 41 (2012) 7108-7146.

[13] C. Florindo, L.C. Branco, I.M. Marrucho, Development of hydrophobic deep eutectic solvents for extraction of pesticides from aqueous environments, Fluid Phase Equilib. 448 (2017) 135-142.

[14] B.D. Ribeiro, C. Florindo, L.C. Iff, M.A.Z. Coelho, I.M. Marrucho, Menthol-based Eutectic Mixtures: Hydrophobic Low Viscosity Solvents, ACS Sustainable Chemistry & Engineering 3 (2015) 2469-2477.

[15] P. Bonhote, A.P. Dias, M. Armand, N. Papageorgiou, K. Kalyanasundaram, M. Gratzel, Hydrophobic, highly conductive ambient-temperature molten salts (vol 35, pg 1168, 1996), Inorg. Chem. 37 (1996) 166-166.

[16] A. Yadav, J.R. Kar, M. Verma, S. Naqvi, S. Pandey, Densities of aqueous mixtures of (choline chloride+ethylene glycol) and (choline chloride+malonic acid) deep eutectic solvents in temperature range 283.15–363.15K, Thermochim. Acta 600 (2015) 95-101.

[17] A.R. Harifi-Mood, R. Buchner, Density, viscosity, and conductivity of choline chloride + ethylene glycol as a deep eutectic solvent and its binary mixtures with dimethyl sulfoxide, J. Mol. Liq. 225 (2017) 689-695.

[18] D. Lapeña, L. Lomba, M. Artal, C. Lafuente, B. Giner, Thermophysical characterization of the deep eutectic solvent choline chloride:ethylene glycol and one of its mixtures with water, Fluid Phase Equilib. 492 (2019) 1-9.

[19] F.S. Mjalli, O.U. Ahmed, Ethaline and Glyceline binary eutectic mixtures: characteristics and intermolecular interactions, Asia-Pac. J. Chem. Eng. 12 (2017) 313-320.

[20] H. Shekaari, M.T. Zafarani-Moattar, M. Mokhtarpour, S. Faraji, Volumetric and compressibility properties for aqueous solutions of choline chloride based deep eutectic solvents and Prigogine–Flory–

Patterson theory to correlate of excess molar volumes at T = (293.15 to 308.15) K, J. Mol. Liq. 289 (2019).
[21] H. Shekaari, M. Taghi Zafarani-Moattar, M. Mokhtarpour, S. Faraji, Compatibility of sustainable solvents ionic liquid, 1-ethyl-3-methylimidazolium ethyl sulfate in some choline chloride based deep eutectic solvents: thermodynamics study, J. Chem. Thermodyn. 141 (2020) 105961.
[22] H. Shekaari, M.T. Zafarani-Moattar, M. Mokhtarpour, S. Faraji, Volumetric and compressibility properties for aqueous solutions of choline chloride based deep eutectic solvents and Prigogine–Flory–Patterson theory to correlate of excess molar volumes at T = (293.15 to 308.15) K, J. Mol. Liq. 289 (2019) 111077.
[23] F. Chemat, H. Anjum, A.M. Shariff, P. Kumar, T. Murugesan, Thermal and physical properties of (Choline chloride + urea +l-arginine) deep eutectic solvents, J. Mol. Liq. 218 (2016) 301-308.
[24] R. Khalil, N. Chaabene, M. Azar, I.B. Malham, M. Turmine, Effect of the chain lengthening on transport properties of imidazolium-based ionic liquids, Fluid Phase Equilib. 503 (2020) 112316.
[25] Z. Gu, J.F. Brennecke, Volume Expansivities and Isothermal Compressibilities of Imidazolium and Pyridinium-Based Ionic Liquids, J. Chem. Eng. Data 47 (2002) 339-345.
[26] C. Caleman, P.J. van Maaren, M. Hong, J.S. Hub, L.T. Costa, D. van der Spoel, Force Field Benchmark of Organic Liquids: Density, Enthalpy of Vaporization, Heat Capacities, Surface Tension, Isothermal Compressibility, Volumetric Expansion Coefficient, and Dielectric Constant, J Chem Theory Comput 8 (2012) 61-74.
[27] E.A. Crespo, J.M.L. Costa, A.M. Palma, B. Soares, M.C. Martín, J.J. Segovia, P.J. Carvalho, J.A.P. Coutinho, Thermodynamic characterization of deep eutectic solvents at high pressures, Fluid Phase Equilib. 500 (2019).
[28] N.F. Gajardo-Parra, M.J. Lubben, J.M. Winnert, Á. Leiva, J.F. Brennecke, R.I. Canales, Physicochemical properties of choline chloride-based deep eutectic solvents and excess properties of their pseudo-binary mixtures with 1-butanol, J. Chem. Thermodyn. 133 (2019) 272-284.
[29] N.S.M. Vieira, I. Vázquez-Fernández, J.M.M. Araújo, N.V. Plechkova, K.R. Seddon, L.P.N. Rebelo, A.B. Pereiro, Physicochemical Characterization of Ionic Liquid Binary Mixtures Containing 1-Butyl-3-methylimidazolium as the Common Cation, J. Chem. Eng. Data 64 (2019) 4891-4903.
[30] J.F. Kincaid, H. Eyring, A.E. Stearn, The Theory of Absolute Reaction Rates and its Application to Viscosity and Diffusion in the Liquid State, Chem. Rev. 28 (1941) 301-365.
[31] H. Eyring, Viscosity, plasticity, and diffusion as examples of absolute reaction rates, J. Chem. Phys. 4 (1936) 283-291.
[32] G.B. Appetecchi, M. Montanino, D. Zane, M. Carewska, F. Alessandrini, S. Passerini, Effect of the alkyl group on the synthesis and the electrochemical properties of N-alkyl-N-methyl-pyrrolidinium bis(trifluoromethanesulfonyl)imide ionic liquids, Electrochim. Acta 54 (2009) 1325-1332.
[33] H. Shirota, A.M. Funston, J.F. Wishart, E.W. Castner, Jr., Ultrafast dynamics of pyrrolidinium cation ionic liquids, J. Chem. Phys. 122 (2005) 184512.
[34] M. Galiński, A. Lewandowski, I. Stępniak, Ionic liquids as electrolytes, Electrochim. Acta 51 (2006) 5567-5580.
[35] A.J. Bard, L.R. Faulkner, J. Leddy, C.G. Zoski, Electrochemical methods: fundamentals and applications. wiley New York, 1980.